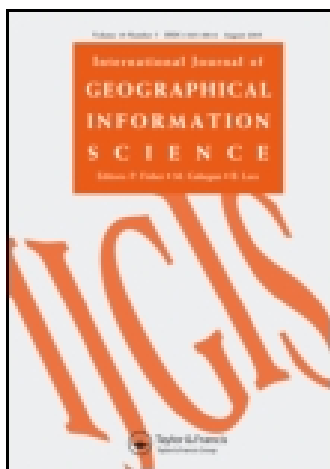


This article was downloaded by: [Tulane University]

On: 08 October 2014, At: 06:29

Publisher: Taylor & Francis

Informa Ltd Registered in England and Wales Registered Number: 1072954 Registered office: Mortimer House, 37-41 Mortimer Street, London W1T 3JH, UK



International Journal of Geographical Information Science

Publication details, including instructions for authors and subscription information:

<http://www.tandfonline.com/loi/tgis20>

Free advanced modeling and remote-sensing techniques for wetland watershed delineation and monitoring

Javier Martínez-López, María F. Carreño^a, José A. Palazón-Ferrando^a, Julia Martínez-Fernández^a & Miguel A. Esteve^a

^a Ecology and Hydrology Department, Faculty of Biology, University of Murcia, Murcia E-30100, Spain

Published online: 05 Dec 2013.

To cite this article: Javier Martínez-López, María F. Carreño, José A. Palazón-Ferrando, Julia Martínez-Fernández & Miguel A. Esteve (2014) Free advanced modeling and remote-sensing techniques for wetland watershed delineation and monitoring, International Journal of Geographical Information Science, 28:8, 1610-1625, DOI: [10.1080/13658816.2013.852677](https://doi.org/10.1080/13658816.2013.852677)

To link to this article: <http://dx.doi.org/10.1080/13658816.2013.852677>

PLEASE SCROLL DOWN FOR ARTICLE

Taylor & Francis makes every effort to ensure the accuracy of all the information (the "Content") contained in the publications on our platform. However, Taylor & Francis, our agents, and our licensors make no representations or warranties whatsoever as to the accuracy, completeness, or suitability for any purpose of the Content. Any opinions and views expressed in this publication are the opinions and views of the authors, and are not the views of or endorsed by Taylor & Francis. The accuracy of the Content should not be relied upon and should be independently verified with primary sources of information. Taylor and Francis shall not be liable for any losses, actions, claims, proceedings, demands, costs, expenses, damages, and other liabilities whatsoever or howsoever caused arising directly or indirectly in connection with, in relation to or arising out of the use of the Content.

This article may be used for research, teaching, and private study purposes. Any substantial or systematic reproduction, redistribution, reselling, loan, sub-licensing, systematic supply, or distribution in any form to anyone is expressly forbidden. Terms &

Free advanced modeling and remote-sensing techniques for wetland watershed delineation and monitoring

Javier Martínez-López*, María F. Carreño, José A. Palazón-Ferrando,
Julia Martínez-Fernández and Miguel A. Esteve

Ecology and Hydrology Department, Faculty of Biology, University of Murcia, Murcia E-30100, Spain

(Received 28 May 2013; accepted 2 October 2013)

Watershed scale studies focusing on hydrological pressures influencing freshwater ecosystem dynamics are necessary for the establishment of suitable wetland ecological indicators. Enhanced and reproducible methods for watershed modeling and land-cover assessment are thus essential tools for wetland monitoring and management. However, few integrated studies propose advanced open source methodologies for watershed modeling and assessment. In this study, a set of GIS methodological tools was applied and further developed in order to delineate wetland watersheds and map their land-cover changes over time. Watersheds draining to 11 semiarid Mediterranean saline wetlands were delimited and map algebra operations were applied on the digital elevation model in the Campo de Cartagena coastal plain to enhance watershed delimitation. land-use/land-cover maps of wetland watersheds were obtained for years 1987 and 2008 by means of supervised classification of Landsat images. A set of four spectral indices was included in the classification analysis using a combination of bands in order to improve the discrimination of vegetation, water bodies, infrastructure, and bare soil. An iterative classification procedure based on maximum likelihood and random selection of training areas was applied. Contextual information based on automatic image segmentation of Landsat scenes was also included as ancillary layers. Watershed areas obtained ranged from 70 to 17,000 ha and delineation was improved in the Campo de Cartagena coastal plain. The proposed image classification methodology showed high accuracies and improved standard classification techniques. The proposed methodology is based on free and open source tools, which makes it broadly applicable.

Keywords: wetlands; watershed; hydrological modeling: Free and open source software; remote sensing

1. Introduction

Wetlands naturally act as a sink of upland-occurring drainage (Ji 2008). Land-use changes lead to hydrological alterations at the watershed level, which directly influence biotic communities in freshwater and terrestrial ecosystems (Tong and Chen 2002, Carreño *et al.* 2008). The expansion of agricultural irrigated areas and urban and tourist development in the Mediterranean Region, and more specifically in Murcia province (SE Spain), during recent decades has led to relevant hydrological changes that affect watersheds and their associated wetland ecosystems (Esteve *et al.* 2008). Long-term monitoring of land uses/cover at watershed scale is therefore highly important for the proper establishment of

*Corresponding author. Email: javier.martinez@um.es

indicators of wetland condition (Roth *et al.* 1996, McHugh *et al.* 2007). However, few integrated studies propose advanced free open source methodologies for wetland watershed modeling and assessment (Aspinall and Pearson 2000, Hollenhorst *et al.* 2007, Zhou *et al.* 2008).

Delineating specific watershed areas draining to each wetland with high accuracy is essential for the establishment of landscape–wetland relationships, especially in relation to landscape hydrological processes (Felicísimo 1994, Hollis and Thompson 1998, Turner *et al.* 2003). However, standard GIS hydrological modeling modules are not always suitable for proper watershed delineation (Baker *et al.* 2006, Callow *et al.* 2007). Watersheds are usually delineated by the area upstream from a given outlet point. Therefore, when several stream network channels drain into a wetland, their respective outlet points within the wetland area must be accurately located in proper relationship to streams and the flow direction map. Especially in flat areas, identifying relevant outlet points inside the wetland area can be a very time-consuming process, particularly for large wetlands. Enhanced watershed delineation methods must be applied in coastal plain areas, where the drainage network might not be clearly defined in a digital elevation model (DEM), in order to obtain accurate results.

Several methodological issues arise when performing land-use/land-cover mapping by means of supervised classification methods (Lu and Weng 2007, Horning *et al.* 2010). Distinctiveness of spectral signatures for each land-use/land-cover class depends on the available remote sensor bands. However, available bands can be also combined into several indices, which enhance the discrimination of land-cover classes (Zha *et al.* 2003). Standard available classification methods do not account for neighboring pixels. However, landscapes consist of several land-cover class patches, often bigger than image pixel size. Pixel-based classification methods are highly dependent on pixel size and usually lead to a large amount of isolated pixels of different land-cover classes in the resulting map (Stuckens *et al.* 2000, Smith and Fuller 2001). Landscape patches of the same land-cover class tend to have similar shapes, e.g., urban and agricultural areas tend to be geometric whereas natural areas are irregular. Recent studies have applied image segmentation for similar applications, such as forest-cover mapping (Magnussen *et al.* 2004, Hay *et al.* 2005, Hirata and Takahashi 2011). Thus, contextual information is needed to enhance pixel-based classification methods when generating landscape maps (Yan *et al.* 2006, Blaschke 2010, Vieira *et al.* 2012). The selection of reliable and representative training site sets is also crucial for the proper elaboration of spectral signatures, thus determining classification accuracy. This is especially important for land-cover time series maps, for which training sites must be extracted from different sources, often of unequal quality. Since older aerial photographs have lower resolution, reliable training sites are more difficult to obtain.

Free and open source software (FOSS) GIS provides advanced environmental modeling and management tools and is becoming widely used in terms of number of projects, end users, and financial support (Steiniger and Bocher 2009). This study offers an enhanced procedure for the monitoring of watershed pressures on wetlands by means of a better delineation of specific watershed areas and the accurate assessment of their land-use changes by means of FOSS.

The objective of this study was to develop and apply a set of enhanced methods to delineate 11 semiarid Mediterranean saline wetland watersheds in Murcia province and to map their land uses in 1987 and 2008 by combining hydrological modeling and remote sensing using FOSS. Our specific objectives were: (1) to accurately establish wetland watersheds, improving delineation methods in plain areas and for large wetlands; (2) to

map land uses in wetland watersheds in years 1987 and 2008 by means of an improved procedure of supervised image classification that (a) uses several spectral indices to enhance discrimination of land-cover classes, (b) includes patch scale information in image classification, and (c) minimizes the effect of training site intraclass heterogeneity.

2. Materials and methods

2.1. Study area

Murcia province (SE Spain: 37° N, 1° W) has a semiarid Mediterranean climate with a mean annual temperature of 16 °C and a mean annual precipitation of 339 mm (Esteve *et al.* 2006). Eleven semiarid saline wetlands were selected, i.e., seven coastal and four inland wetlands (Figure 1). Selected sites are included in the regional inventory of wetlands (Vidal-Abarca *et al.* 2003) and their protection status ranges from regional, national to international level due to their high ecological values (Ramsar Site, Special Protection Area for Birds, Site of Community Importance and Special Protection Area for the Mediterranean), except for Matalentisco and Boquera de Tabala wetlands, which do not benefit from any protection status. Marina del Carmol, Lo Poyo, and Playa de la Hita wetlands are in a lowland coastal plain, called Campo de Cartagena, associated with the internal shore of the Mar Menor coastal lagoon which comprises 12,700 ha (Conesa and Jiménez-Cárceles 2007). The Campo de Cartagena coastal plain comprises 1275 km² is under the influence of a very arid climate with a mean annual temperature higher than



Figure 1. Wetland location map in Murcia province (SE Spain). Wetland keys: **H1**: Rasall; **CR3**: Cañada Brusca; **CR10**: Carmoli; **CR5**: Alcanara; **CR14**: Ajauque; **CR13**: Lopoyo; **CR15**: Derramadores; **CR19**: Boquera de Tabala; **CR20**: Playa de la Hita; **CR4**: Matalentisco; **CR21**: Sombrerico.

18°C and mean annual rainfall under 300 mm (Conesa 1990). The lagoon and its associated wetlands are all RAMSAR sites, containing 18 Habitats of Community Interest according to the European Habitat Directive (Council of Europe 1992). Salinas del Rasall is a coastal wetland associated with a salt extraction pond embedded in the Calblanque Natural Park, and also included in the Mar Menor RAMSAR protected area. Matalentisco, Sombrerico, and Cañada Brusca are coastal wetlands located in the southern part of the region on the Mediterranean Sea. Boquera de Tabala, Ajauque, Derramadores, and Alcanara are inland wetlands associated with an ephemeral river and with a saline alluvial plain, respectively.

2.2. Digital elevation model preprocessing and delimitation of wetland watersheds

A 10 m resolution DEM of Murcia province created by the Instituto Geográfico Nacional was used for hydrological modeling. Map layers and GIS analyses have been processed with GRASS GIS 6.4 software (GRASS Development Team 2008, Neteler *et al.* 2012). Map algebra operations were applied on the DEM in the Campo de Cartagena coastal plain to reinforce the existing drainage network and to force flow accumulation from all draining areas around wetland perimeter to converge into a single point within the wetland area. A pixel in an arbitrary coordinate within each wetland area was first selected, which ultimately served as a sink or outlet point, from which to delineate the wetland watershed. Then, a wetland map was created in which remaining pixels inside wetland area were assigned a distance value related to the selected pixel. From this map, a new map was created calculating the inverse distances, showing the highest value in the pixel selected as a sink. This map was then subtracted from the raw 10 m resolution DEM of the Campo de Cartagena. Therefore, a single point was obtained within the wetland area from which to perform watershed delineation in order to collect all drainage fluxes reaching the wetland perimeter. Outside of wetland areas, the DEM was also modified by lowering the elevation values coinciding with the existing ephemeral stream network to force flow-direction models to match existing stream lines (Figure 2; Olaya Ferrero 2004, King *et al.* 2005). This is a so-called 'stream burning' operation. The drainage network in the Campo de Cartagena coastal plain was thus forced to match the existing stream network. For the delineation of the remaining wetland watersheds outside the Campo de Cartagena area, the raw DEM was used.

Maps of flow accumulation and drainage direction based on the DEM were generated using the single flow direction (D8 algorithm). For wetlands in the Campo de Cartagena area, two main inflows coming from the watersheds were obtained, which converged into the previously selected sink point (Figure 3). Watersheds were finally delimited from the selected sink coordinates within the wetlands using the drainage direction maps.

2.3. Remote sensing of watershed land use/land cover

The Landsat sensor was selected as a suitable image data source due to its medium spatial resolution and high spectral and temporal resolution provided that: (1) medium spatial resolution is appropriate for regional scale studies; (2) high spectral resolution enhances the discrimination of land-cover types; and (3) high temporal resolution allowed us to add phenological information to the classification analysis in order to better discriminate some land-cover classes using two images for each study year. Map layers and GIS and statistical analyses in this study have been processed with GRASS GIS 6.4 software and R (R Core Team 2012).

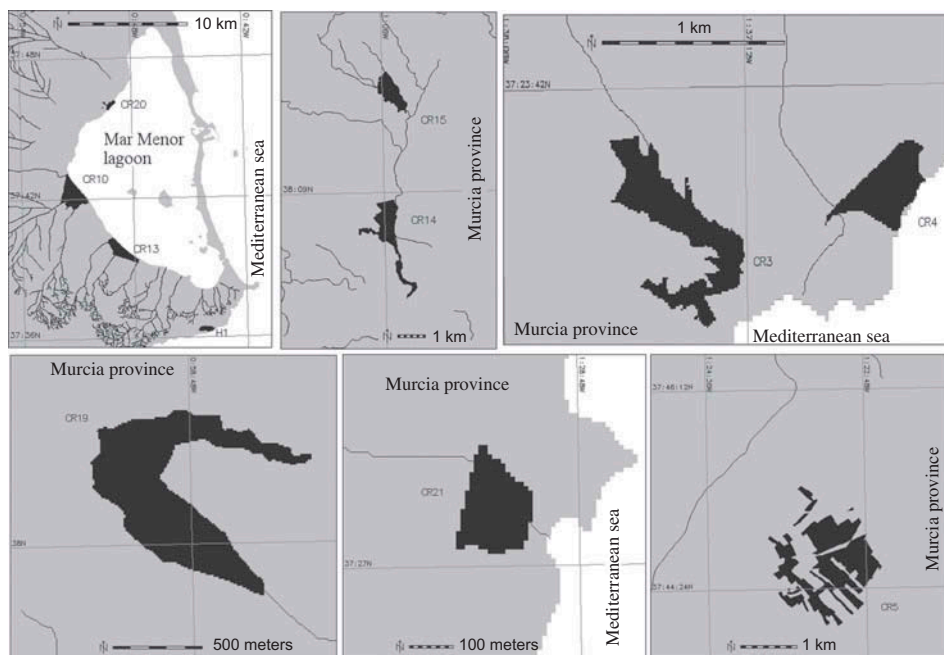


Figure 2. Wetland maps in relation to the ephemeral river network. Wetland keys: **H1**: Rasall; **CR3**: Cañada Brusca; **CR10**: Carmoli; **CR5**: Alcanara; **CR14**: Ajauque; **CR13**: Lopoyo; **CR15**: Derramadores; **CR19**: Boquera de Tabala; **CR20**: Playa de la Hita; **CR4**: Matalentisco; **CR21**: Sombrerico.

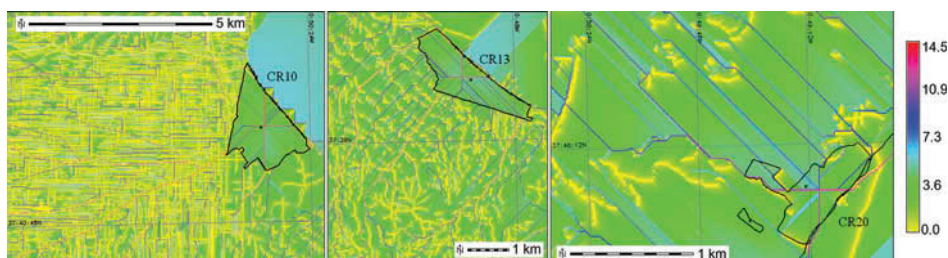


Figure 3. Detail of resulting maps of flow accumulation (log scaled) at the Campo the Cartagena wetlands. Left: Marina del Carmoli wetland (CR10); center: Lopoyo wetland (CR13); right: Playa de la Hita wetland (CR20).

Landsat 4 images were used for the classification in 1987, corresponding to the TM sensor, while the ETM+ sensor was used (Landsat 7) for the 2008 classification. Spectral bands used were: blue (B), green (G), red (R), near infrared (NIR), and short-wave infrared (MIR). Pixel size was set to 25 m. Two Landsat images corresponding to different dates, winter and late spring, were used for each classification in order to account for the changing seasonal phenology of vegetation during the dry and wet periods (Bradley and Mustard 2005). Landsat images from 1987 and 2008 were obtained from the Instituto Universitario del Agua y del Medio Ambiente and from the Instituto Geográfico Nacional, respectively. Atmospheric correction of images was performed using the dark-object

subtraction technique (Chavez 1988, 1996, Chander *et al.* 2009). Eleven land-cover classes were mapped in years 1987 and 2008: (1) dense (DNW) and (2) open (ONW) natural woodland, (3) dense (DNS) and (4) open (ONS) natural shrubland, (5) dry arboreal (DAC) and (6) herbaceous (DHC) cropland, (7) irrigated arboreal (IAC) and (8) herbaceous (IHC) cropland, (9) greenhouses (GHs), (10) unproductive land and infrastructure (INF), and (11) water bodies (WBs).

2.3.1. Spectral indices

Four spectral indices for each Landsat image were calculated and were included in the classification analysis as ancillary layers. These indices enhance the discrimination of vegetation, urban areas, bare soil, and WBs. The normalized differential vegetation index (NDVI) was calculated (Rouse *et al.* 1973). NDVI is widely used in remote-sensing studies for the identification of vegetation since it highlights photosynthetic activity (Bannari *et al.* 1995). Dense vegetation shows NDVI values closed to one, soil values are positive but lower, and water values are negative due to its strong absorption at NIR (Glenn *et al.* 2008). The modified normalized difference water index (MNDWI; Hui *et al.* 2008) was calculated to delineate WBs and enhance its presence. This index can also remove shadow effects on water, which are otherwise difficult to detect. The normalized difference built-up index (NDBI; Zha *et al.* 2003) was calculated to enhance the discrimination of built-up areas. Finally, we calculated the normalized difference bareness index (NDBaI; Chen *et al.* 2006). This index retrieves bare soil from the Landsat images. Bare soil (including beaches, bare soil, and land under development) could be distinguished by NDBaI values greater than zero.

2.3.2. Contextual information

Landscape patches in the study area were extracted by means of automatic segmentation performed on a single Landsat scene for each year using *SPRING 5.1.5* software (Camara *et al.* 1996; see figure 4). *Region Growing* data segmentation technique was performed on image bands number 1–7 (excluding the thermal infrared band). Similarity threshold (ranging from 0% to 100%) and minimum patch size (in image pixels units) parameters were set to 20 and 100 respectively, following experimentation. Two shape indices for each obtained patch were then calculated and scores were assigned to pixels belonging to each patch. The new maps with each corresponding shape index values were included in the classification as ancillary layers, hence including patch information at pixel scale. Patches from the resulting map were scored according to the shape indices. Two new maps were created based on fractal dimension (FD) and shape index (SI) of patches sensu Chust and Ducrot (2004), which were used as ancillary input layers for classification.

2.3.3. Supervised classification: the random classifier method

land-use/land-cover maps were obtained by supervised classification using the maximum likelihood algorithm (Michelson *et al.* 2000, Richards and Jia 2006). Input data for the classification analysis were the resulting shape and spectral indices maps, together with the single bands of the two Landsat scenes except for the thermal infrared band, which was not included in the analysis. Training and validation sites were obtained through aerial photograph interpretation. Classification was enhanced with an iterative procedure that minimizes the effect of uncertainty and heterogeneity in the selection of training sites,



Figure 4. Automated landscape patches map obtained with *SPRING* software. Different colors represent different landscape patches.

called ‘randomclasiter’. This procedure was developed by Carreño *et al.* (2011) and the code is available online (<https://github.com/Paquicf/randomclasiter>). The procedure combines *GRASS*, *R*, and bash scripts to automatically perform several supervised classifications, randomly selecting a different subset of training areas each time. For the 2008 classification, a total of 521 training areas were selected from an aerial image of Murcia Region from year 2008 (DGPNB 2008) using QGIS software (Development-Team 2009). For the 1987 classification, a total of 407 training areas were selected from an aerial image of Murcia Region from year 1987 from the Confederación Hidrográfica del Segura. One hundred iterations were performed and for each of them 25–50% of the training areas were randomly selected. This percentage was the same across iterations but different for each land-cover class, depending on the total number of training sites available.

In each classification, a pixel might be assigned to different land-cover classes, depending on the set of training areas selected. One hundred maps were therefore generated and later summarized into 11 maps – one for each land-cover class, each of them representing the total frequency of assignment of each pixel to a specific land-cover class, ranging from 0 to 100 (i.e., the number of iterations). The final land-cover class assigned to a pixel in the resulting map was ultimately the class which was most often assigned to this pixel.

The methodology was verified by aerial image validation and stratified random sampling by land-cover class. The number of pixels used to validate each land-cover class was proportional to the number of training sites. A total of 696 pixels were used as validation areas for year 2008 and 636 pixels for year 1987. Classification results were validated by means of the *Overall Accuracy* parameter and the *Kappa* coefficient

(Chuvieco 2002, Foody 2002). User's and producer's accuracy parameters were also calculated for each land-cover class of interest (Congalton 1991).

3. Results

3.1. Wetland watershed delimitation enhancements

Watershed areas obtained ranged from 70 to 17,000 ha (see supplementary kml files and Table 1). In the Campo de Cartagena coastal plain area derived watersheds were consistent with previous hydrological studies and were larger than the ones obtained without DEM preprocessing (Figure 5; Conesa 1990). Results showed that in Cañada Brusca wetland, two different wetland areas were drained by distinct watersheds, thus presenting different hydrological influences at watershed scale. Therefore, the wetland was divided into two different sites: Cañada Brusca North (CR3N) and South (CR3S).

3.2. Image classification enhancements

Overall accuracy percentages and kappa values for the 1987 and 2008 classifications were higher using the randomclaster methodology in relation to the standard method (Table 2),

Table 1. Wetland and resulting watershed areas (ha).

Wetland	Wetland area	Watershed area
Humedal de las Salinas del Rasall	26.3	236
Saladar de Cañada Brusca South	3.8	69.5
Saladar de Cañada Brusca North	17.4	360
La Alcanara	199	6508
Marina del Carmoli	314	16,923
Playa de la Hita	34.4	2052.8
Saladar de Matalentisco	10.4	907.6
Saladar de la Boquera de Tabala	36.9	5819.2
Lopoyo	80	2783
Ajauque	100	7792
Derramadores	50	1963
Sombrerico	3	141

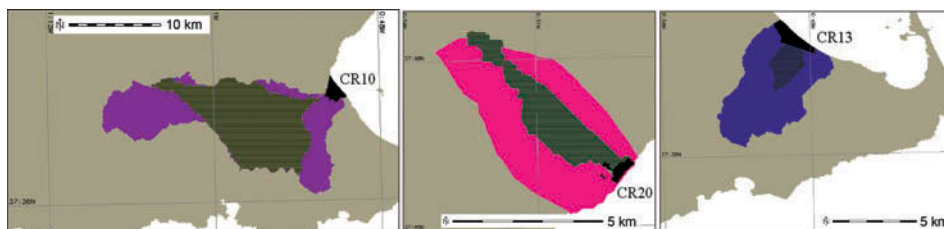


Figure 5. Resulting wetland watersheds in the Campo de Cartagena coastal plain. Wetland areas are represented in black. Resulting watershed areas obtained without DEM preprocessing are represented with dashed lines and final watershed areas (using DEM preprocessing) are in different colors. Left: Marina del Carmoli wetland (CR10); center: Lopoyo wetland (CR13); right: Playa de la Hita wetland (CR20).

Table 2. Comparison of overall accuracy and kappa coefficients of classifications in 1987 and 2008 after the standard and enhanced classification methodology.

	1987		2008	
	Overall accuracy	Kappa	Overall accuracy	Kappa
Standard methodology	64.87%	0.61	77.19%	0.75
Enhanced methodology	72.51%	0.69	83.01%	0.81

showing higher values in 2008 than in 1987. The inclusion of a set of spectral indices as ancillary layers clearly improved the proper classification of pixels (Figure 6b) in relation to using only the NDVI (Figure 6a), and the inclusion of shape indices (Figure 6c) resulted in less and more compact landscape patches. The randomclasiter method enhanced classification (Figure 6d) and the best results were obtained combining all methodologies (Figure 6e) in terms of overall accuracy and landscape patch identification. The combined enhanced classification method resulted in a 40% reduction in the number of landscape patches in comparison with the standard methodology and maximum patch size increased by three times. Results from the accuracy analysis by land-cover class showed that high user's and producer's accuracies were generally obtained in the 1987 and 2008 classifications (Table 3). As a whole, natural land-cover classes (DNW, ONW, DNS, and ONS) were accurately assessed in both years, as well as WBs. Dry farmed areas

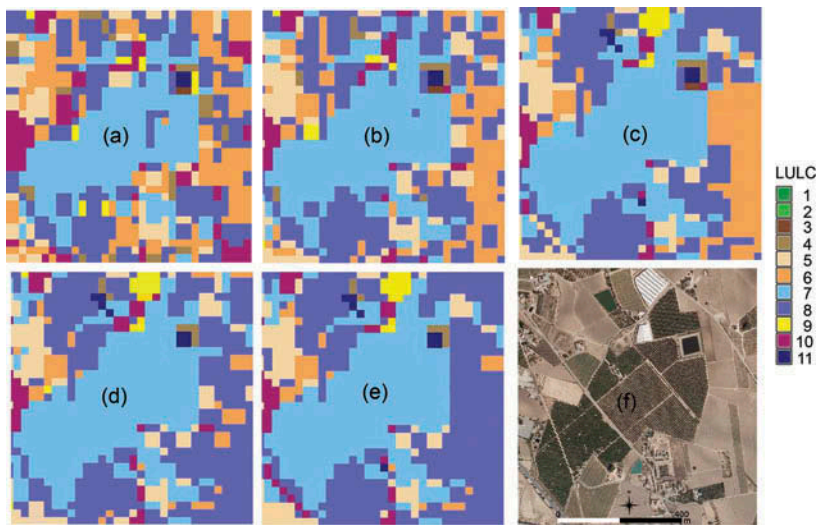


Figure 6. Detail of classification maps using different methodologies: (a) standard maximum likelihood (ML) classification method including only NDVI as spectral index, (b) standard ML classification method including all spectral indices, (c) standard ML classification method including spectral indices and contextual information (d) iterative training selection procedure including spectral indices, (e) iterative training selection procedure including spectral indices and contextual information, (f) aerial picture of the study area. Key of land-cover classes: 1: dense and 2: open natural woodland; 3: dense and 4: open natural shrubland; 5: dry arboreal; and 6: herbaceous cropland; 7: irrigated arboreal and 8: herbaceous cropland; 9: greenhouses; 10: unproductive land and infrastructure; and 11: water bodies.

Table 3. Accuracy coefficients (%) of classification maps for each land-cover class in 1987 and 2008 using the enhanced methodology. Land-cover classes key: dense (DNW) and open (ONW) natural woodland, dense (DNS) and open (ONS) natural shrubland, dry arboreal (DAC) and herbaceous (DHC) cropland, irrigated arboreal (IAC) and herbaceous (IHC) cropland, greenhouses (GHs), infrastructure (INF) and water bodies (WBs).

	1987		2008	
	User's accuracy	Producer's accuracy	User's accuracy	Producer's accuracy
DNW	84.62	78.57	80.80	86.79
ONW	71.05	71.05	54.87	86.01
DNS	62.27	75.71	78.24	69.38
ONS	68.99	78.18	70.03	51.32
DAC	90.52	63.25	48.23	81.90
DHC	71.08	70.77	50.79	85.16
IAC	48.33	90.00	94.83	88.75
IHC	62.50	84.75	88.59	69.26
GHs	80.00	57.14	91.59	93.90
INF	95.65	57.89	91.20	95.21
WBs	98.32	98.67	100.00	98.76

(DAC and DHC) were partially overrepresented in the 2008 classification, as well as irrigated crops (IAC and IHC) in 1987. Conversely, GHs and INF were slightly under-represented in the 1987 classification.

3.3. Watershed land-cover changes

Land-cover maps in 1987 and 2008 were obtained for all wetland watersheds, except for those which were only studied in 2008, i.e., Lopoyo (CR13), Derramadores (CR15), Ajauque (CR14), and Sombrerico (CR21) wetlands. Land-cover classes of wetland watersheds mapped both years showed an increase in irrigated areas, except for Cañada Brusca South and Rasall wetland watersheds which did not show irrigated areas during the study period (Figure 7). In 1987, dry farmed areas were predominant in the watersheds of Marina del Carmolí, Boquera de Tabala, and Alcanara wetlands, while natural areas were the predominant land-cover class in the watersheds of Cañada Brusca North and South, Matalentisco, and Rasall wetlands. Wetland watersheds mapped only in 2008 showed high percentages of irrigated areas. As an example, resulting land-cover maps for the Marina del Carmolí wetland watershed are in Figures 8 and 9.

4. Discussion

This study proposes enhanced free and open source hydrological modeling and image classification procedures, supporting landscape ecology studies in relation to environmental modeling and monitoring (Newton *et al.* 2009). Previous studies on wetlands located in the Campo de Cartagena coastal plain did not provide specific watershed areas for the study sites but rather focused on the whole Campo de Cartagena catchment area (Carreño *et al.* 2008, Esteve *et al.* 2008). However, this methodology was successfully applied and tested in several studies, allowing the assessment of specific pressures for each wetland site studied (Martínez-López *et al.* 2012, Martínez-López *et al.* 2014a, 2014b).

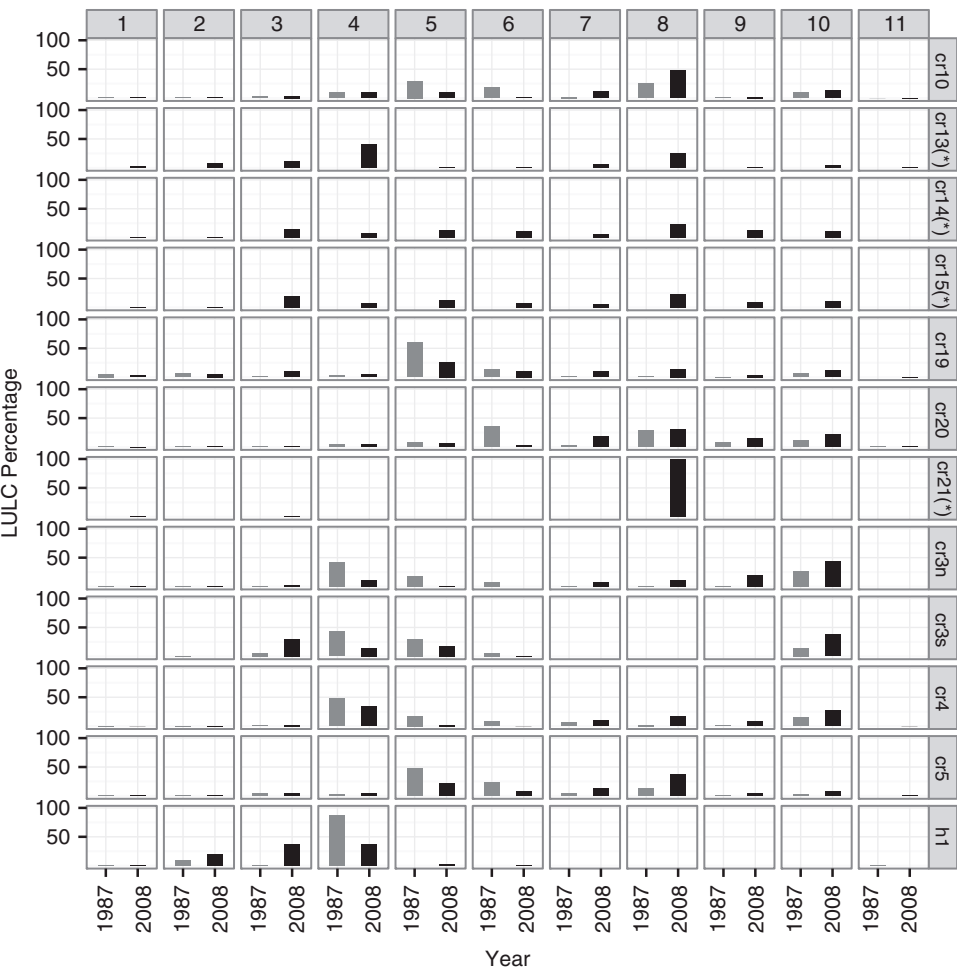


Figure 7. Land-use/land-cover changes in wetland watersheds during the study period. Key of land-cover classes: **1**: dense and **2**: open natural woodland; **3**: dense and **4**: open natural shrubland; **5**: dry arboreal; and **6**: herbaceous cropland; **7**: irrigated arboreal and **8**: herbaceous cropland; **9**: greenhouses; **10**: unproductive land and infrastructure and **11**: water bodies. Wetland keys: **H1**: Rasall; **CR3N**: Cañada Brusca North; **CR3S**: Cañada Brusca South; **CR10**: Carmoli; **CR5**: Alcanara; **CR14**: Ajauque; **CR13**: Lopoyo; **CR15**: Derramadores; **CR19**: Boquera de Tabala; **CR20**: Playa de la Hita; **CR4**: Matalentisco; **CR21**: Sombrerico. Wetland watersheds denoted with an asterisk show only land- cover values for year 2008.

Following the proposed methodology, landscape patches are much better identified and higher accuracies are obtained in the resulting land-use/land-cover maps in comparison with the standard supervised classification. However, standard accuracy measures might not sufficiently reflect these enhancements since they are pixel-based (Duro *et al.* 2012). The applied hydrological correction methods successfully improved calculation of watershed areas in wetlands located in plain areas and for some complex wetlands like Cañada Brusca, which receive different surface hydrological influences. As a way to resolve flow direction in flat areas, the DEM stream burning pre-processing together with the creation of sinks within wetland areas served for the proper delineation of wetland

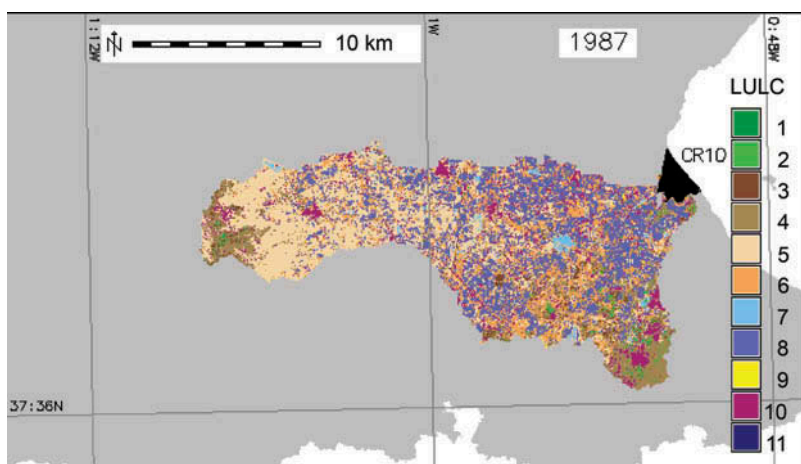


Figure 8. Land-use/land-cover maps in Marina del Carmolí wetland watershed (CR10) in 1987. Key of land-cover classes: **1:** dense and **2:** open natural woodland; **3:** dense and **4:** open natural shrubland; **5:** dry arboreal and **6:** herbaceous cropland; **7:** irrigated arboreal and **8:** herbaceous cropland; **9:** greenhouses; **10:** unproductive land and infrastructure and **11:** water bodies.

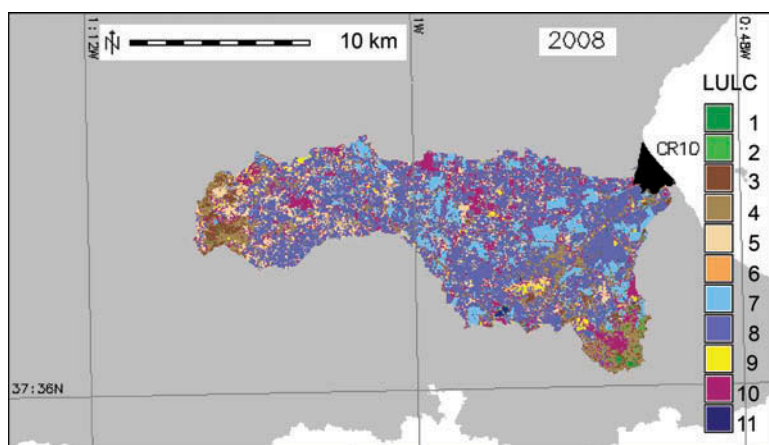


Figure 9. Land-use/land-cover maps in Marina del Carmolí wetland watershed (CR10) in 2008. Key of land-cover classes: **1:** dense and **2:** open natural woodland; **3:** dense and **4:** open natural shrubland; **5:** dry arboreal and **6:** herbaceous cropland; **7:** irrigated arboreal and **8:** herbaceous cropland; **9:** greenhouses; **10:** unproductive land and infrastructure; and **11:** water bodies.

watersheds. Even though parallel flow paths were obtained due to the single flow direction algorithm used (D8), globally, the flow went toward the ephemeral river network cells. Therefore, the use of multiple flow direction algorithms, like D-Infinity, could enhance flow path maps in flat areas (Tarboton 1997).

By means of the randomclaster procedure, the problem of the representativeness of training sites was minimized, resulting in higher map accuracies. This is especially the case in the 1987 land-use/land-cover classification maps due to the lower resolution of older aerial photographs, which increased uncertainty in training site selection. This

iterative method contributes to the existing ensemble classification methods, like random forest (Breiman 2001, Gislason *et al.* 2006), allowing the use of parametric classifiers and its direct application under the GRASS GIS environment. This improved image classification methodology can be also applied to analyze pixel thematic uncertainties, based on the number of times that a pixel was assigned to each different category, in relation to spatial and spectral variables (Brown *et al.* 2009).

The use of several spectral indices as ancillary layers enhanced the discrimination of land-cover classes and the inclusion of patch-scale geometric attributes of different land-cover classes resulted in more compact landscape patches (Narumalani *et al.* 1998, Whiteside *et al.* 2011, Aguirre-Gutiérrez *et al.* 2012). *Spring* software, used for image segmentation, is proposed as an effective and free alternative to commercial ones (e.g., *eCognition*). In this study, we tried to use a minimum set of spectral indices which targeted general land-cover classes like vegetation, urban areas, WBs, and bare soil areas. However, some other spectral indices can be used, such as soil-adjusted vegetation index (SAVI; Huete 1988) and MSAVI (Qi *et al.* 1994), especially for semi-arid environments with low vegetation densities, which could enhance classification results.

Overall, irrigated areas increased across wetland watersheds during the study period, except for two of them. Landsat is an appropriate sensor for long-term historical studies due to its several satellite missions since 1972 (Wolter *et al.* 2006). Spatial, temporal, and spectral resolution of Landsat sensors was also suitable for land-cover mapping at a regional scale (Franklin and Wulder 2002).

Results promote the use of FOSS for these kinds of studies, due to their applicability and worldwide free availability (Tufto and Cavallini 2005, Steiniger and Hay 2009). This methodology can be easily further developed and tested with new satellite sensors like the Landsat Data Continuity Mission (Irons *et al.* 2012) and open source image processing algorithms implemented in some libraries in python (Scikit-image Team 2013) and R (Goslee 2011). Furthermore, the proposed method is easily automated by means of bash scripts, thus resulting in a free and effective procedure for wetland watershed assessment and monitoring.

Acknowledgments

The authors acknowledge the comments from Jon Olav Skøien, two anonymous reviewers, and the Editor on an earlier version of the manuscript.

References

- Aguirre-Gutiérrez, J., Seijmonsbergen, A.C., and Duivenvoorden, J.F., 2012. Optimizing land cover classification accuracy for change detection, a combined pixel-based and object-based approach in a mountainous area in Mexico. *Applied Geography*, 34, 29–37.
- Aspinall, R. and Pearson, D., 2000. Integrated geographical assessment of environmental condition in water catchments: linking landscape ecology, environmental modelling and GIS. *Journal of Environmental Management*, 59 (4), 299–319.
- Baker, M.E., Weller, D.E., and Jordan, T.E., 2006. Comparison of automated watershed delineations: effects on land cover areas, percentages, and relationships to nutrient discharge. *Photogrammetric Engineering and Remote Sensing*, 72 (2), 159–168.
- Bannari, A., *et al.*, 1995. A review of vegetation indices. *Remote Sensing Reviews*, 13 (1), 95–120.
- Blaschke, T., 2010. Object based image analysis for remote sensing. *ISPRS Journal of Photogrammetry and Remote Sensing*, 65 (1), 2–16.
- Bradley, B.A. and Mustard, J.F., 2005. Identifying land cover variability distinct from land cover change: cheatgrass in the Great Basin. *Remote Sensing of Environment*, 94 (2), 204–213.

- Breiman, L., 2001. Random forests. *Machine Learning*, 45, 5–32.
- Brown, K.M., Foody, G.M., and Atkinson, P.M., 2009. Estimating perpixel thematic uncertainty in remote sensing classifications. *International Journal of Remote Sensing*, 30 (1), 209–229.
- Cámara, G., et al., 1996. SPRING: integrating remote sensing and GIS by object-oriented data modelling. *Computers & Graphics*, 20 (3), 395–403.
- Callow, J.N., Niel, K.P.V., and Boggs, G.S., 2007. How does modifying a DEM to reflect known hydrology affect subsequent terrain analysis? *Journal of Hydrology*, 332 (12), 30–39.
- Carreño, M.F., et al., 2008. Habitat changes in coastal wetlands associated to hydrological changes in the watershed. *Estuarine Coastal and Shelf Science*, 77 (3), 475–483.
- Carreño, M.F., et al., 2011. Aplicación de nuevas técnicas para la clasificación supervisada de imágenes Landsat en la determinación de usos del suelo: por píxel y por mancha. *Mapping Interactivo*, marzo-abril, 68–73.
- Chander, G., Markham, B.L., and Helder, D.L., 2009. Summary of current radiometric calibration coefficients for Landsat MSS, TM, ETM+, and EO-1 ALI sensors. *Remote Sensing of Environment*, 113 (5), 893–903.
- Chavez, P.S., 1988. An improved dark-object subtraction technique for atmospheric scattering correction of multispectral data. *Remote Sensing of Environment*, 24 (3), 459–479.
- Chavez, P.S., 1996. Image-based atmospheric corrections revisited and improved. *Photogrammetric Engineering and Remote Sensing*, 62 (9), 1025–1036.
- Chen, X.L., et al., 2006. Remote sensing image-based analysis of the relationship between urban heat island and land use/cover changes. *Remote Sensing of Environment*, 104 (2), 133–146.
- Chust, G. and Ducrot, D., 2004. Land cover mapping with patch-derived landscape indices. *Landscape and Urban Planning*, 69, 437–449.
- Chuvieco, E., 2002. *Teledetección ambiental. la observación de la tierra desde el espacio. 1*. Barcelona: Editorial Ariel.
- Conesa, C., 1990. *El Campo de Cartagena: clima e hidrología en un medio semiárido. I Cuadernos*. Vol. 13. Murcia: Universidad de Murcia.
- Conesa, H.M. and Jiménez-Cárceles, F.J., 2007. The Mar Menor lagoon (SE Spain): a singular natural ecosystem threatened by human activities. *Marine Pollution Bulletin*, 54 (7), 839–849.
- Congalton, R.G., 1991. A review of assessing the accuracy of classifications of remotely sensed data. *Remote Sensing of Environment*, 37 (1), 35–46.
- R Core Team, 2012. *R: A Language and Environment for Statistical Computing*. Vienna, Austria.
- Council of Europe, 1992. Council Directive 92/43/EEC of 21 May 1992 on the conservation of natural habitats and of wild fauna and flora. *Official Journal L*, 206 (22/07), 7–50.
- Development-Team, 2009. *Quantum GIS Geographic Information System. Open Source Geospatial Foundation Project*.
- DGPNB, 2008. *Consejería de Agricultura y Agua. Comunidad Autónoma de la Región de Murcia. NATMUR-08 project*. Available from: <http://www.murcianatural.com/natmur08/> [Accessed 22 October 2013].
- Duro, D.C., Franklin, S.E., and Dubé, M.G., 2012. A comparison of pixel-based and object-based image analysis with selected machine learning algorithms for the classification of agricultural landscapes using SPOT-5 HRG imagery. *Remote Sensing of Environment*, 118, 259–272.
- Esteve, M.A., et al., 2006. Los ecosistemas de la Región de Murcia: componentes, estructura y dinámica. In: C. Conesa, Ed., *El medio físico de la Región de Murcia*. Murcia: EDITUM. Universidad de Murcia, 245–278.
- Esteve, M.A., et al., 2008. Dynamics of Coastal Wetlands and Land Use Changes in the Watershed: Implications for the Biodiversity. In: R.E. Russo, Ed., *Wetlands: Ecology, Conservation and Restoration*. Hauppauge, NY: Nova Science, chap. 4, 133–175.
- Felícísimo, A.M., 1994. *Modelos digitales del terreno*. Oviedo: Pentalfa.
- Foody, G.M., 2002. Status of land cover classification accuracy assessment. *Remote Sensing of Environment*, 80 (1), 185–201.
- Franklin, S.E. and Wulder, M.A., 2002. Remote sensing methods in medium spatial resolution satellite data land cover classification of large areas. *Progress in Physical Geography*, 26 (2), 173–205.
- Gislason, P.O., Benediktsson, J.A., and Sveinsson, J.R., 2006. Random Forests for land cover classification. *Pattern Recognition Letters*, 27 (4), 294–300.

- Glenn, E.P., *et al.*, 2008. Relationship between remotely-sensed vegetation indices, canopy attributes and plant physiological processes: what vegetation indices can and cannot tell us about the landscape. *Sensors*, 8 (4), 2136–2160.
- Goslee, S.C., 2011. Analyzing remote sensing data in R: the Landsat package. *Journal of Statistical Software*, 43 (4), 1–25.
- GRASS Development Team, 2008. *Geographic Resources Analysis Support System Software*. Available from: <http://grass.fbk.eu> [Accessed 22 October 2013].
- Hay, G.J., *et al.*, 2005. An automated object-based approach for the multiscale image segmentation of forest scenes. *International Journal of Applied Earth Observation and Geoinformation*, 7 (4), 339–359.
- Hirata, Y. and Takahashi, T., 2011. Image segmentation and classification of Landsat thematic mapper data using a sampling approach for forest cover assessment. This article is one of a selection of papers from Extending Forest Inventory and Monitoring over Space and Time. *Canadian Journal of Forest Research*, 41 (1), 35–43.
- Hollenhorst, T.P., *et al.*, 2007. Methods for generating multi-scale watershed delineations for indicator development in Great Lake Coastal Ecosystems. *Journal of Great Lakes Research*, 33 (3), 13–26.
- Hollis, G.E. and Thompson, J.R., 1998. Hydrological data for wetland management. *Water and Environment Journal*, 12 (1), 9–17.
- Horning, N., *et al.*, 2010. *Remote sensing for ecology and conservation: a handbook of techniques*. Oxford University Press.
- Huete, A., 1988. A soil-adjusted vegetation index (SAVI). *Remote Sensing of Environment*, 25 (3), 295–309.
- Hui, F., *et al.*, 2008. Modelling spatial-temporal change of Poyang Lake using multitemporal Landsat imagery. *International Journal of Remote Sensing*, 29 (19–20), 18.
- Irons, J.R., Dwyer, J.L., and Barsi, J.A., 2012. The next Landsat satellite: the Landsat data continuity mission. *Remote Sensing of Environment*, 122, 11–21.
- Ji, W., 2008. *Wetland and water resource modeling and assessment: a watershed perspective*. Boca Raton, FL: CRC Press.
- King, R.S., *et al.*, 2005. Spatial considerations for linking watershed land cover to ecological indicators in streams. *Ecological Applications*, 15 (1), 137–153.
- Lu, D. and Weng, Q., 2007. A survey of image classification methods and techniques for improving classification performance. *International Journal of Remote Sensing*, 28 (5), 823–870.
- Magnussen, S., Boudewyn, P., and Wulder, M., 2004. Contextual classification of Landsat TM images to forest inventory cover types. *International Journal of Remote Sensing*, 25 (12), 2421–2440.
- Martínez-López, J., *et al.*, 2014a. Wetland and landscape indices for assessing the condition of semiarid Mediterranean saline wetlands under agricultural hydrological pressures. *Ecological Indicators*, 36, 400–408.
- Martínez-López, J., *et al.*, 2014b. Remote sensing of plant communities as a tool for assessing the condition of semiarid Mediterranean saline wetlands in agricultural catchments. *International Journal of Applied Earth Observation and Geoinformation*, 26, 193–204.
- Martínez-López, J., Carreño, M., and Esteve-Selma, M., 2012. Índice de estado ecológico de criptohumedales semiáridos en relación con la protección de sus cuencas. In: M. Angel Esteve-Selma, Ed., *Los espacios naturales protegidos de la Región de Murcia: estudio de casos desde una perspectiva interdisciplinar*. Murcia: Editum, 157–180.
- McHugh, O.V., *et al.*, 2007. Integrated qualitative assessment of wetland hydrological and land cover changes in a data scarce dry Ethiopian highland watershed. *Land Degradation & Development*, 18 (6), 643–658.
- Michelson, D.B., Liljeberg, B.M., and Pilesjö, P., 2000. Comparison of algorithms for classifying Swedish landcover using Landsat TM and ERS-1 SAR data. *Remote Sensing of Environment*, 71 (1), 1–15.
- Narumalani, S., Zhou, Y., and Jelinski, D.E., 1998. Utilizing geometric attributes of spatial information to improve digital image classification. *Remote Sensing Reviews*, 16 (4), 233–253.
- Neteler, M., *et al.*, 2012. GRASS GIS: A multi-purpose open source GIS. *Environmental Modelling & Software*, 31 (0), 124–130.
- Newton, A.C., *et al.*, 2009. Remote sensing and the future of landscape ecology. *Progress in Physical Geography*, 33 (4), 528–546.

- Olaya Ferrero, V., 2004. Hidrología Computacional y Modelos Digitales de Terreno: Teoría, práctica y filosofía de una nueva forma de análisis hidrológico. Available online at: http://www.gabrielortiz.com/descargas/Hidrologia_Computacional_MDT_SIG.pdf.
- Qi, J., et al., 1994. A modified soil adjusted vegetation index. *Remote Sensing of Environment*, 48 (2), 119–126.
- R Core Team, 2012. *R: A Language and Environment for Statistical Computing*. Vienna, Austria.
- Richards, J.A. and Jia, X., 2006. *Remote Sensing Digital Image Analysis: An Introduction*. 4th Springer.
- Roth, N.E., Allan, J.D., and Erickson, D.L., 1996. Landscape influences on stream biotic integrity assessed at multiple spatial scales. *Landscape Ecology*, 11 (3), 141–156.
- Rouse, J.W., et al., 1974. Monitoring vegetation systems in the Great Plains with ERTS. In: S.C. Freden, E.P. Mercanti, and M.A. Becker, (eds.), *Proceedings of the Third ERTS Symposium, Volume I: Technical Presentations*. NASA SP-351. NASA, Washington DC, 309–317.
- Scikit-image Team, 2013. *Scikit-image 0.8.0*. Available from: <http://scikit-image.org> [Accessed 22 October 2013].
- Smith, G.M. and Fuller, R.M., 2001. An integrated approach to land cover classification: an example in the Island of Jersey. *International Journal of Remote Sensing*, 22 (16), 3123–3142.
- Steiniger, S. and Bocher, E., 2009. An overview on current free and open source desktop GIS developments. *International Journal of Geographical Information Science*, 23 (10), 1345–1370.
- Steiniger, S. and Hay, G.J., 2009. Free and open source geographic information tools for landscape ecology. *Ecological Informatics*, 4 (4), 183–195.
- Stuckens, J., Coppin, P., and Bauer, M., 2000. Integrating contextual information with per-pixel classification for improved land cover classification. *Remote Sensing of Environment*, 71 (3), 282–296.
- Tarboton, D.G., 1997. A new method for the determination of flow directions and upslope areas in grid digital elevation models. *Water Resources Research*, 33 (2), 309–319.
- Tong, S.T.Y. and Chen, W., 2002. Modeling the relationship between land use and surface water quality. *Journal of Environmental Management*, 66 (4), 377–393.
- Tufto, J. and Cavallini, P., 2005. Should wildlife biologists use free software? *Wildlife Biology*, 11 (1), 67–76.
- Turner, R.K., et al., 2003. Towards an integrated environmental assessment for wetland and catchment management. *The Geographical Journal*, 169 (2), 99–116.
- Vidal-Abarca, M.R., et al., 2003. Los humedales de la Región de Murcia: Claves para su interpretación. Consejería de Agricultura, Agua y Medio Ambiente. Dirección General del Medio Natural, Murcia.
- Vieira, M.A., et al., 2012. Object based image analysis and data mining applied to a remotely sensed Landsat time-series to map sugarcane over large areas. *Remote Sensing of Environment*, 123, 553–562.
- Whiteside, T.G., Boggs, G.S., and Maier, S.W., 2011. Comparing object-based and pixel-based classifications for mapping savannas. *International Journal of Applied Earth Observation and Geoinformation*, 13 (6), 884–893.
- Wolter, P., Johnston, C., and Niemi, G., 2006. Land use land cover change in the US Great Lakes basin 1992 to 2001. *Journal of Great Lakes Research*, 32 (3), 607–628.
- Yan, G., et al., 2006. Comparison of pixelbased and objectoriented image classification approachesa case study in a coal fire area, Wuda, Inner Mongolia, China. *International Journal of Remote Sensing*, 27 (18), 4039–4055.
- Zha, Y., Gao, J., and Ni, S., 2003. Use of normalized difference built-up index in automatically mapping urban areas from TM imagery. *International Journal of Remote Sensing*, 24 (3), 583–594.
- Zhou, D., Gong, H., and Liu, Z., 2008. Integrated ecological assessment of biophysical wetland habitat in water catchments: linking hydro-ecological modelling with geo-information techniques. *Ecological Modelling*, 214 (24), 411–420.